American Mineralogist, Volume 88, pages 37–46, 2003

An infrared spectroscopic study of the basic copper phosphate minerals: Cornetite, libethenite, and pseudomalachite

WAYDE MARTENS AND RAY L. FROST*

Centre for Instrumental and Developmental Chemistry, Queensland University of Technology, GPO Box 2434, Brisbane, Queensland 4001, Australia

ABSTRACT

The molecular structures of the basic copper phosphate minerals pseudomalachite, libethenite, and cornetite were studied using a combination of infrared emission spectroscopy, infrared absorption, and Raman spectroscopy. Infrared emission spectra of these minerals were obtained over the temperature range 100 to 1000 °C.

The infrared spectra of the three minerals are different, in line with differences in crystal structure and composition. The absorption spectra are similar, particularly in the OH stretching region, but characteristic differences in the bending regions are observed. Differences are also observed in the phosphate stretching and bending regions. The IR emission of the basic copper phosphates studied shows that the minerals are completely dehydroxylated by 550 °C.

INTRODUCTION

Several dark green copper phosphate minerals are known to exist, including pseudomalachite [$Cu_5(PO_4)_2(OH)_4$], (Anthony et al. 2000) and its polymorphs reichenbachite and ludjibaite (Braithwaite and Ryback 1994; Hyrsl 1991; Lhoest 1995; Sieber et al. 1987). The relative stabilities of the basic copper phosphates have been determined using estimated chemical parameters (Moore 1984) and experimentally determined solubility products are available (Williams 1990). Normal Cu^{2+} phosphate is not known as a naturally occurring mineral. As expected, the more basic stoichiometries occupy fields at higher pH. Pseudomalachite is the stable phase under chemical conditions intermediate to those that serve to stabilize libethenite and cornetite. Paragenetic relationships have been explored (Williams 1990). Such relationships are important as these minerals can occur as corrosion products in copper piping carrying potable water.

Pseudomalachite is monoclinic, space group $P2_1/a$ (Piret and Deliens 1988). Pseudomalachite is isomorphous with cornwallite (refined in different setting with a and c interchanged, space group $P2_1/c$). The pseudomalachite crystal structure contains one P atom in the asymmetric unit (total of 2 in the cell). Each phosphorus atom is bonded to 4 crystallographically independent O atoms. There are two crystallographically independent OH ions. These minerals occur in the oxidized zones of copper deposits and pseudomalachite is by far the most common (Anthony et al. 2000). It is frequently accompanied by libethenite [$Cu_2PO_4(OH)$], which is monoclinic, space group $P2_1/n$ (Anthony et al. 2000). The multiplicity of atoms associated with the phosphate group is the same as for pseudomalachite, with four formula units in the unit cell. There is one crystallographically independent OH group in the unit cell (total of four). A rarer congener is cornetite [$Cu_3PO_4(OH)_3$] (orthorhombic, space group *Pbca*). There is one unique P atom in the asymmetric unit (eight in the unit cell) bonded to four independent O atoms. There are three crystallographically independent OH ions in the unit cell.

The structure of the above-mentioned minerals may be explored at the molecular level using vibrational spectroscopy. Farmer (1974) reported the infrared absorption spectra of libethenite, cornetite, and pseudomalachite. Raman spectra can provide information as to the symmetry of the molecular species and to position, or energy of the bands. The Raman spectra of aqueous phosphate anions show the symmetric stretching mode (ν_1) at 938 cm^{-1}, the symmetric bending mode (ν_2) at 420 cm^{-1}, the antisymmetric stretching mode (ν_3) at 1017 cm^{-1}, and the ν_4 mode at 567 cm^{-1}. The pseudomalachite vibrational spectrum consists of ν_1 at 953, ν_2 at 422 and 450 cm^{-1}, ν_3 at 1025 and 1096, and ν_4 at 482, 530, 555, and 615 cm^{-1} (Farmer 1974). Libethenite vibrational modes occur at 960 (ν_1), 445 (ν_2), 1050 (ν_3), and 480, 522, 555, 618, and 637 cm^{-1} (ν_4) (Farmer 1974). Cornetite vibrational modes occur at 960 (ν_1), 415 and 464 (ν_2), 1000, 1015, and 1070 (ν_3), and 510, 527, 558, 582, 623, and 647 cm^{-1} (ν_4). Vibrational spectra of reichenbachite and ludjibaite have not as yet been reported.

Phosphate mineral formation is important in corrosion and leaching studies. Minerals can form in zones of secondary oxidation. As part of a comprehensive study of the IR and Raman properties of minerals containing oxygen anions, we report changes in the molecular structure as a function of temperature of the three basic copper phosphate minerals: pseudomalachite, libethenite, and cornetite as determined using infrared emission spectroscopy.

* E-mail: r.frost@qut.edu.au

EXPERIMENTAL METHODS

The minerals were obtained from Australian sources and were checked for purity by X-ray diffraction. The pseudomalachite originated from the West Bogan Mine, Tottenham, New South Wales and also from the Burra Burra Mine, Mt. Lofty Ranges, South Australia. The libethenite also originated from the Burra Burra Mine. The cornetite was obtained from the Blockade Mine, near Mount Isa, Queensland, Australia.

Absorption spectra using KBr pellets were obtained using a Perkin-Elmer Fourier transform infrared spectrometer (2000) equipped with a TGS detector. Spectra were recorded by accumulating 1024 scans at 4 cm^{-1} resolution in the mid-IR over the 400 to 4000 cm^{-1} range.

Fourier transform infrared emission spectroscopy was carried out on a Nicolet spectrometer equipped with a TGS detector, which was modified by replacing the IR source with an emission cell. A description of the cell and principles of the emission experiment have been published elsewhere (Frost et al. 1995, 1999a, 1999b; Frost and Vassallo 1996, 1997; Kloprogge and Frost 1999, 2000a, 2000b). Approximately 0.2 mg of finely ground basic copper phosphate mineral was spread as a thin layer (approximately 0.2 mircometers) on a 6 mm diameter platinum surface and held in an inert atmosphere within a nitrogen-purged cell during heating. Apart from milling the mineral no other sample preparation was involved. The sample simply rests on the Pt holder.

Three sets of spectra were obtained: (1) the black body radiation at selected temperatures, (2) the platinum plate radiation at the same temperatures, and (3) the spectra from the platinum plate covered with the sample. Only one set of black body and platinum radiation is required for each temperature. These sets of data were then used for each mineral. One set of blackbody and Pt data were collected per analytical session. The emittnce spectrum (E) at a particular temperature was calculated by subtraction of the single-beam spectrum of the platinum backplate (Pt) from that of the platinum + sample (S), with the result ratioed to the single beam spectrum of an approximate blackbody (C-graphite). The following equation, which provides comparative sets of data on an absorption-like scale, was used to calculate the emission spectra:

$$E = -0.5 \cdot \log \frac{\mathrm{Pt} - \mathrm{S}}{\mathrm{Pt} - \mathrm{C}}$$

The emission spectra were collected at intervals of 50 °C over the range 200–750 °C. The time between scans (while the temperature was raised to the next hold point) was approximately 100 seconds. It was thought that this was sufficient time for the heating block and the powdered sample to reach thermal equilibrium. The spectra were acquired by coaddition of 64 scans at each temperature (approximate scanning time 45 seconds), with a nominal resolution of 4 cm^{-1}. Good quality spectra can be obtained providing the sample thickness is not too large. If too large a sample is used then the spectra become difficult to interpret because of the presence of combination and overtone bands. Spectral manipulation including baseline adjustment, smoothing, and normalization, was performed using the GRAMS software package (Galactic Industries Corporation).

Band component analysis was undertaken using the Jandel "Peakfit" software package, which enabled the type of fitting function to be selected and allows specific parameters to be fixed or varied accordingly. Band fitting was done using a Gauss-Lorentz cross-product function with the minimum number of component bands used for the fitting process. The Gauss-Lorentz ratio was maintained at values greater than 0.7 and fitting was undertaken until reproducible results were obtained with r^2 correlations greater than 0.995. Peaks were selected for the curve fitting procedure based on (1) fitting the least number of peaks; (2) when the r^2 value does not exceed 0.995, an additional peak is added; (3) all parameters of peak fitting are allowed to vary.

RESULTS AND DISCUSSION

Infrared absorption of the hydroxyl-stretching vibrations

The infrared absorption spectra of the hydroxyl-stretching region of the three phase related basic copper phosphate minerals pseudomalachite, libethenite, and cornetite are shown in Figure 1. Table 1 reports the results of the spectral analysis of these three minerals and compares the results with the Raman data and with infrared data previously published (Farmer 1974; Frost et al. 2002). All three minerals show complex hydroxyl-stretching vibrations. Pseudomalachite infrared spectra display two bands at 3442 and 3388 cm^{-1} of approximately equal intensity with additional broad bands at 3357 and 3199 cm^{-1}. One way of describing these bands is that they represent energy levels of the hydroxyl-stretching modes and the intensity of the bands is a population measurement of the hydroxyl units at any of these energy levels.

These results are in good agreement with our Raman spectra (Frost et al. 2002) in which two bands are observed at 3442 and 3402 cm^{-1}. The results are in excellent agreement with the infrared absorption spectra reported by Farmer (1974). This means that there are two distinct OH units in pseudomalachite.

Curve fitting of the libethenite spectrum shows a single band at 3471 cm^{-1} with a shoulder at 3454 cm^{-1}. The Raman spectrum of the hydroxyl-stretching region of libethenite shows a single band at 3467 cm^{-1}. A shoulder is observed at 3454 cm^{-1}. This is in close agreement with the published IR band observed at 3465 cm^{-1}. This observation implies there are two hydroxyl sites with an unequal distribution of hydroxyl units in libethenite. The infrared absorption spectrum of cornetite contains three bands observed at 3405, 3313, and 3205 cm^{-1} analogous to bands in the Raman spectrum at 3400, 3300, and 3205 cm^{-1}. The infrared absorption spectrum of cornetite is, however, more complex with multiple hydroxyl-stretching vibrations observed. A broad band at around 3360 cm^{-1} may be attributed to adsorbed water.

Infrared absorption of the hydroxyl-bending vibrations

Associated with the hydroxyl-stretching vibrations are the hydroxyl-bending absorption bands. Two infrared absorption bands for pseudomalachite are observed at 810 and 756 cm^{-1}. These bands do not fit into the pattern of the infrared absorption spectra of phosphates and these may be assigned to the hydroxyl-bending modes of the OH unit. Bands are observed

TABLE 1. Vibrational spectroscopic analysis of the infrared spectra of pseudo-malachite, libethenite, and cornetite

Pseudomalachite				Libethenite					Cornetite			
IR Absorption	IES (100 °C)	Raman (Frost et al. 2002)	Published IR data (Farmer 1974)	IR Absorb	IES (100 °C)	Raman (Frost et al. 2002)	Published IR data (Farmer 1974)	Infrared	IES (100 °C)	Raman (Frost et al. 2002)	Published IR data (Farmer 1974)	Suggested assignments
+1 cm^{-1}	+2 cm^{-1}	+1 cm^{-1}		+1 cm^{-1}	+2 cm^{-1}	+1 cm^{-1}		+1 cm^{-1}	+2 cm^{-1}	+1 cm^{-1}	Precision of data	
3442	3440	3442	3582	3454	3464			3405	3411	3400	3285	
3388	3431	3402	3435	3471	3398	3467	3465	3313	3323	3300	3200	OH stretching
	3382		3390					3205	3245	3205		vibration
810	898	877	810	810	819	862	815?	817	887	817	850?	OH bending
756	831	802	762	793		815		773	823	772		vibration
	767	750						750	761	748		
								710				
996	1002	998	953	955	960	975	960	989	1004	994	960	ν_1 Symmetric
978	971	971		917				955		961		stretching
										922		vibration
448		481	450	448		450	445	452		462	464	ν_2 Symmetric
416		451	422	420						433	415	bending
										411		vibration
1095	1101	1084	1096	1031	1056	1050	1050	1093	1053	1054	1070	ν_3 Anti-symmetric
1037	1047	1053	1025			1019		1041			1015	stretching
											1000	vibration
612		609	615	648		645	637	618		570	647	ν_4 Out-of-plane
549		537	555	631		626	618	573		541	623	bending vibration
525		517	530	610		582	555	560		518	582	
478			482	548		556	522			487	558	
							480				527	
											510	

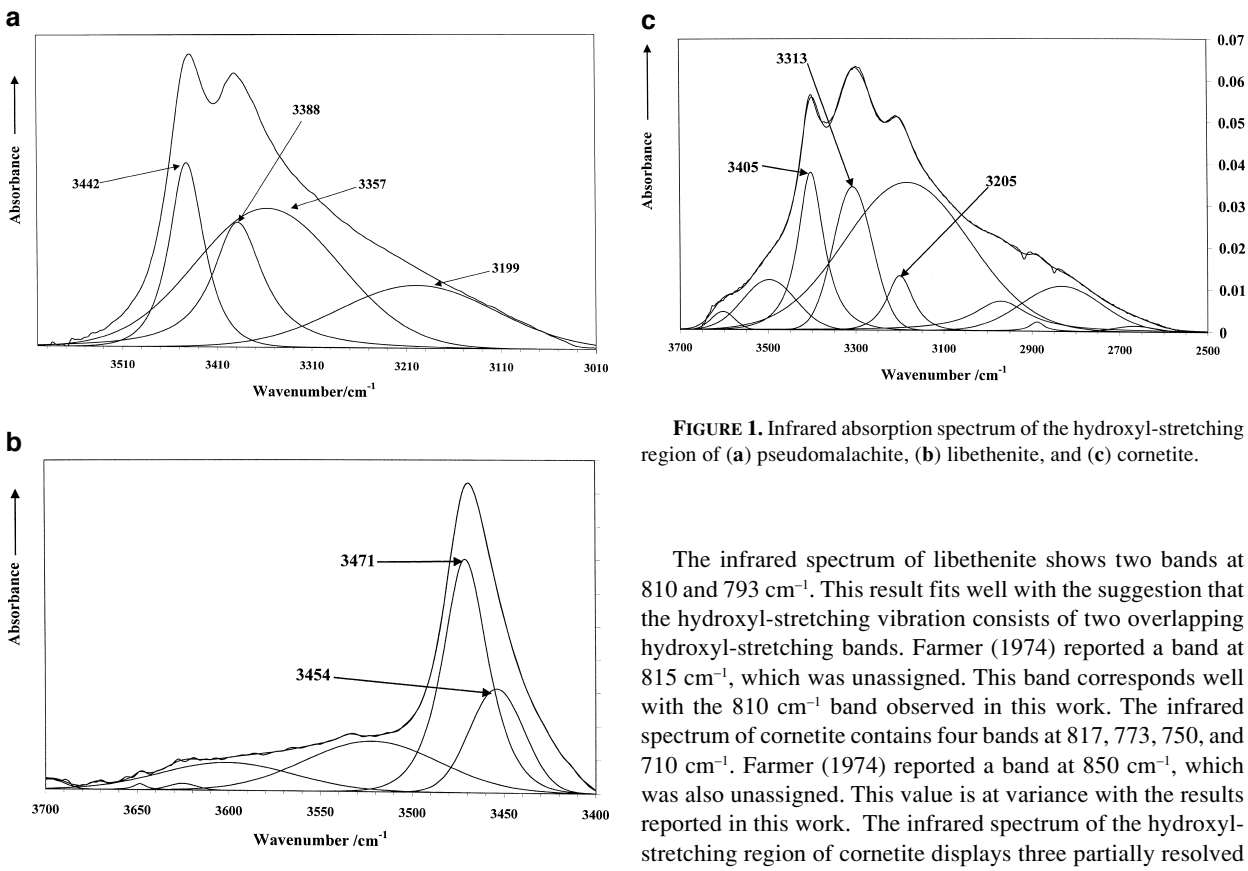

FIGURE 1. Infrared absorption spectrum of the hydroxyl-stretching region of (**a**) pseudomalachite, (**b**) libethenite, and (**c**) cornetite.

in similar positions in the Raman spectra. Two bands were reported by Farmer (1974) at 810 and 762 cm^{-1}, but these were unassigned. The observation of two hydroxyl-bending modes is in agreement with the observation of two hydroxyl-stretching vibrations.

The infrared spectrum of libethenite shows two bands at 810 and 793 cm^{-1}. This result fits well with the suggestion that the hydroxyl-stretching vibration consists of two overlapping hydroxyl-stretching bands. Farmer (1974) reported a band at 815 cm^{-1}, which was unassigned. This band corresponds well with the 810 cm^{-1} band observed in this work. The infrared spectrum of cornetite contains four bands at 817, 773, 750, and 710 cm^{-1}. Farmer (1974) reported a band at 850 cm^{-1}, which was also unassigned. This value is at variance with the results reported in this work. The infrared spectrum of the hydroxyl-stretching region of cornetite displays three partially resolved bands and it is probable that only the first three bands are due to the hydroxyl-bending modes. In the Raman spectrum three bands are observed at 817, 772, and 748 cm^{-1}.

The application of infrared emission spectroscopy to these minerals should allow the correlation of the hydroxyl stretching and bending vibrations and the intensity of these bands as a function of temperature and will assist in the assignment of these bands.

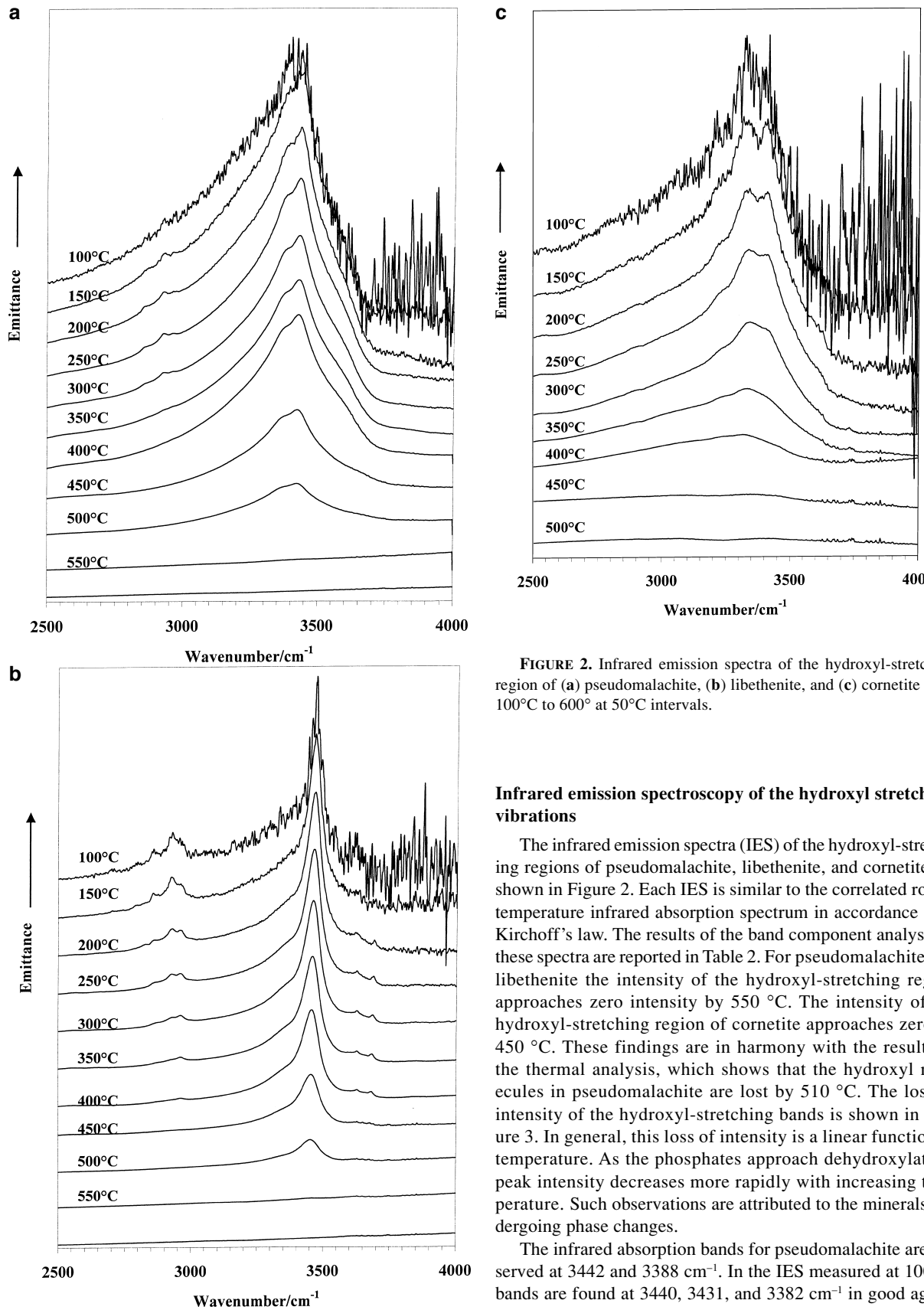

FIGURE 2. Infrared emission spectra of the hydroxyl-stretching region of (**a**) pseudomalachite, (**b**) libethenite, and (**c**) cornetite from 100°C to 600° at 50°C intervals.

Infrared emission spectroscopy of the hydroxyl stretching vibrations

The infrared emission spectra (IES) of the hydroxyl-stretching regions of pseudomalachite, libethenite, and cornetite are shown in Figure 2. Each IES is similar to the correlated room-temperature infrared absorption spectrum in accordance with Kirchoff's law. The results of the band component analysis of these spectra are reported in Table 2. For pseudomalachite and libethenite the intensity of the hydroxyl-stretching region approaches zero intensity by 550 °C. The intensity of the hydroxyl-stretching region of cornetite approaches zero by 450 °C. These findings are in harmony with the results of the thermal analysis, which shows that the hydroxyl molecules in pseudomalachite are lost by 510 °C. The loss of intensity of the hydroxyl-stretching bands is shown in Figure 3. In general, this loss of intensity is a linear function of temperature. As the phosphates approach dehydroxylation, peak intensity decreases more rapidly with increasing temperature. Such observations are attributed to the minerals undergoing phase changes.

The infrared absorption bands for pseudomalachite are observed at 3442 and 3388 cm^{-1}. In the IES measured at 100 °C bands are found at 3440, 3431, and 3382 cm^{-1} in good agree-

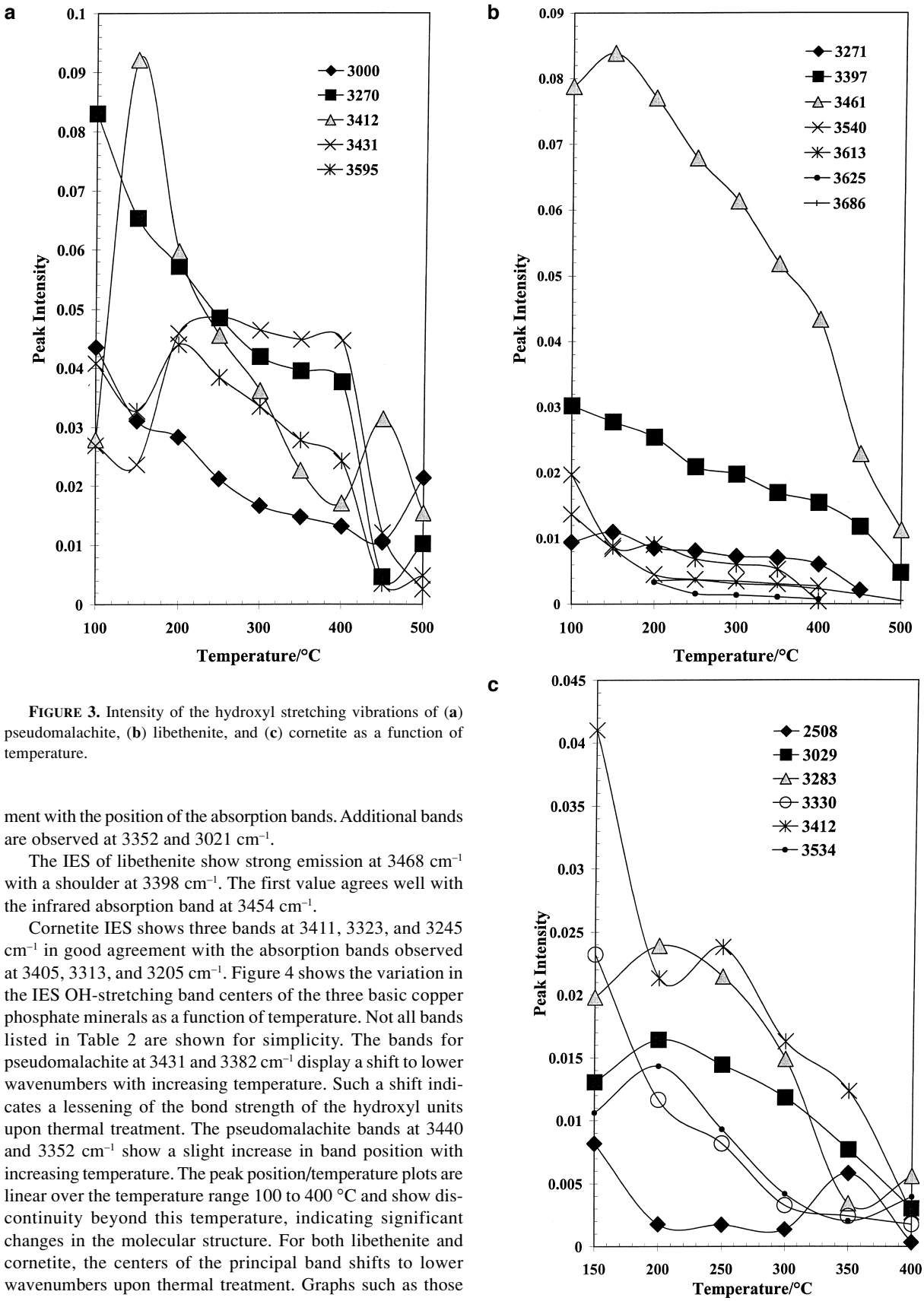

FIGURE 3. Intensity of the hydroxyl stretching vibrations of (**a**) pseudomalachite, (**b**) libethenite, and (**c**) cornetite as a function of temperature.

ment with the position of the absorption bands. Additional bands are observed at 3352 and 3021 cm^{-1}.

The IES of libethenite show strong emission at 3468 cm^{-1} with a shoulder at 3398 cm^{-1}. The first value agrees well with the infrared absorption band at 3454 cm^{-1}.

Cornetite IES shows three bands at 3411, 3323, and 3245 cm^{-1} in good agreement with the absorption bands observed at 3405, 3313, and 3205 cm^{-1}. Figure 4 shows the variation in the IES OH-stretching band centers of the three basic copper phosphate minerals as a function of temperature. Not all bands listed in Table 2 are shown for simplicity. The bands for pseudomalachite at 3431 and 3382 cm^{-1} display a shift to lower wavenumbers with increasing temperature. Such a shift indicates a lessening of the bond strength of the hydroxyl units upon thermal treatment. The pseudomalachite bands at 3440 and 3352 cm^{-1} show a slight increase in band position with increasing temperature. The peak position/temperature plots are linear over the temperature range 100 to 400 °C and show discontinuity beyond this temperature, indicating significant changes in the molecular structure. For both libethenite and cornetite, the centers of the principal band shifts to lower wavenumbers upon thermal treatment. Graphs such as those

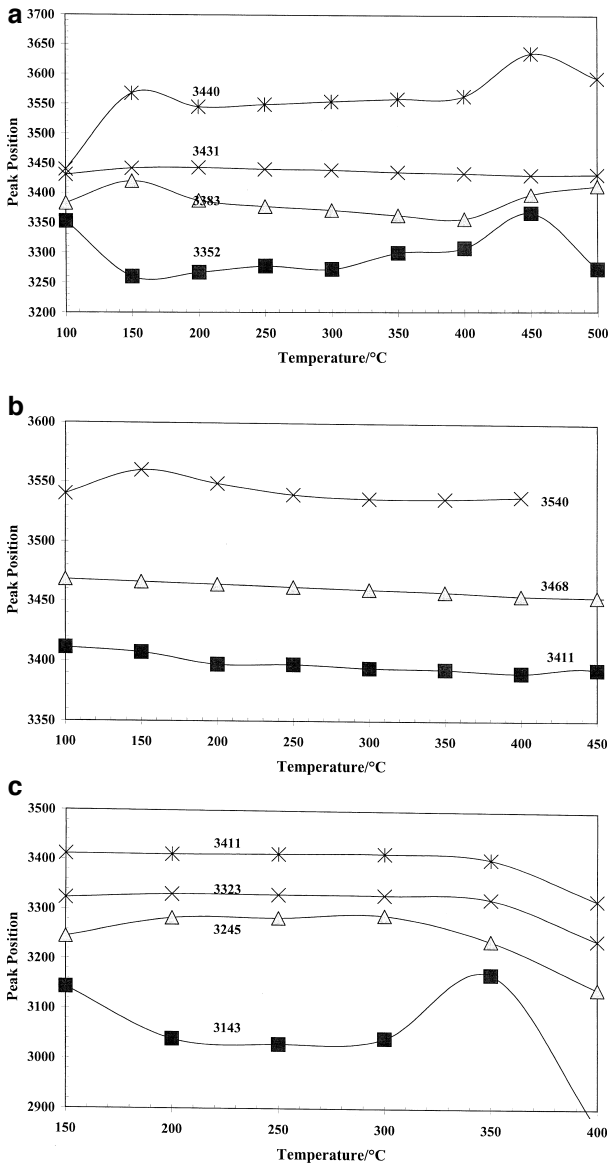

FIGURE 4. Band centers of the hydroxyl stretching vibrations of (**a**) pseudomalachite, (**b**) libethenite, and (**c**) cornetite as a function of temperature.

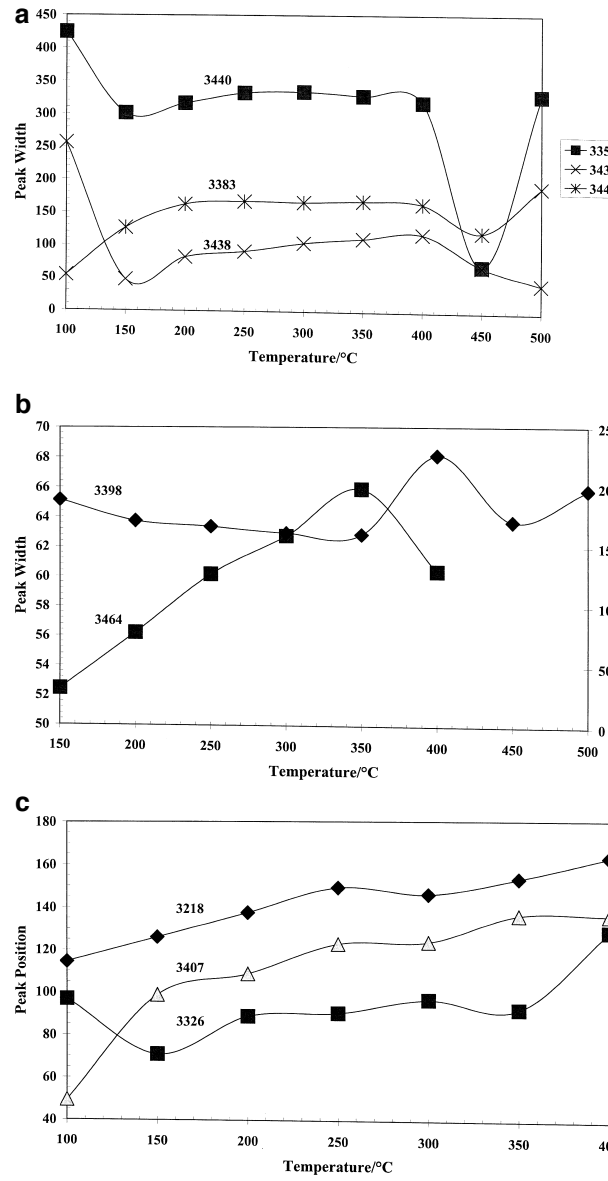

FIGURE 5. Bandwidth of the hydroxyl stretching vibrations of (**a**) pseudomalachite, (**b**) libethenite, and (**c**) cornetite as a function of temperature.

shown in Figure 4 are useful in that (1) the variation in peak position with temperature is observed and in this case the bands moved to lower wavenumbers and (2) discontinuities in the graphs are indicative of phase changes of the phosphates.

Changes in the structure of the phosphates through thermal decomposition may also be explored through changes in the bandwidths of the component peaks in the spectral profile of the hydroxyl-stretching region of the basic copper phosphates.

Figure 5 illustrates the variation in peak width as a function of temperature. In general the peak widths increase with temperature, which means that the structure becomes disordered. An abrupt change is observed in the pseudomalachite peak widths at 450 °C, indicating a change in the molecular structure. The variation of peak width with temperature for libethenite shows similar features except the break in the data is at 300 to 350 °C. This may indicate some thermal decomposition at this point although no variation in band centers was observed (Fig. 5b). Two additional bands, observed only at temperatures above 300 °C, are at 3459 and 3625 cm^{-1}.

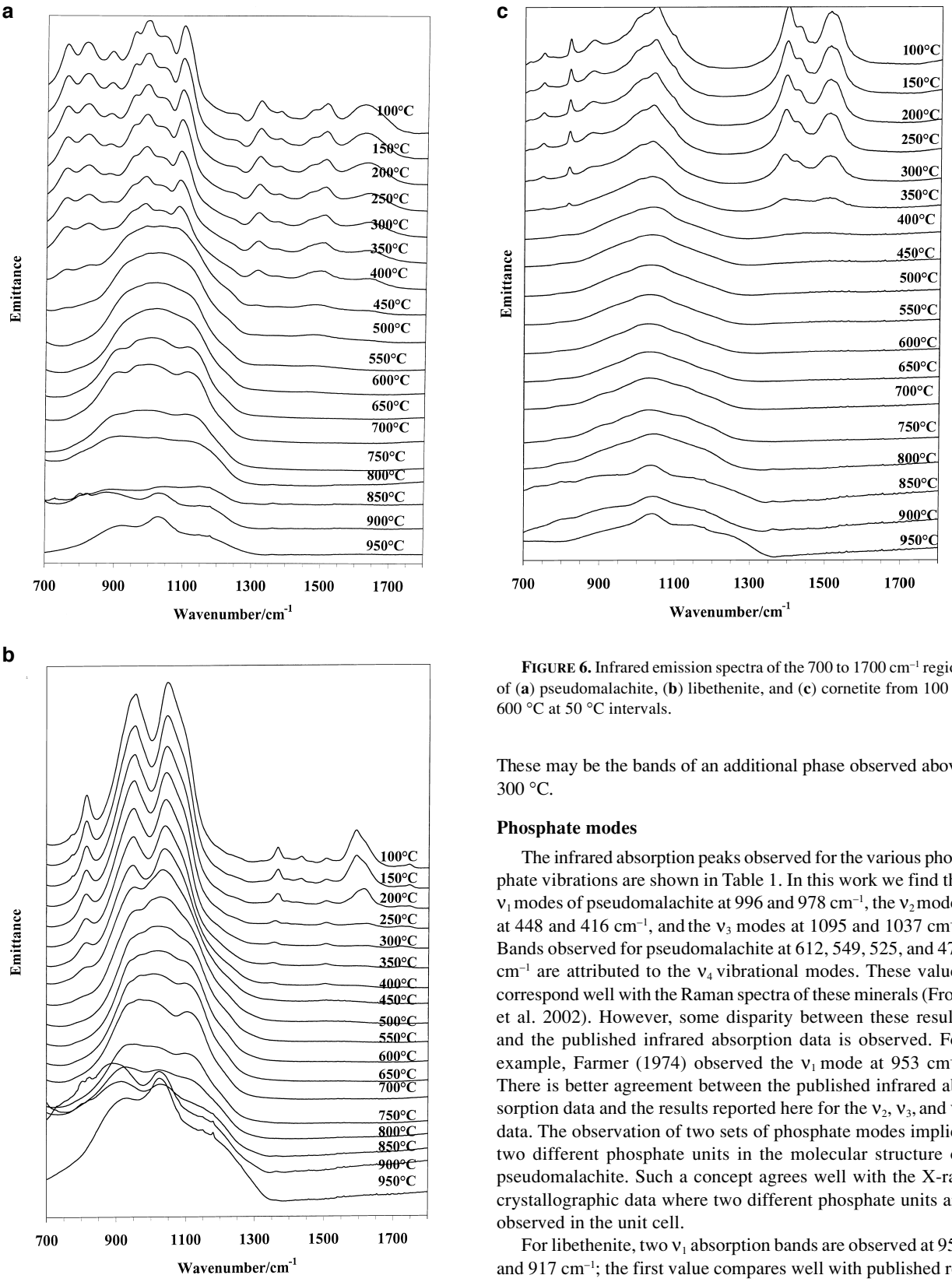

FIGURE 6. Infrared emission spectra of the 700 to 1700 cm^{-1} region of (**a**) pseudomalachite, (**b**) libethenite, and (**c**) cornetite from 100 to 600 °C at 50 °C intervals.

These may be the bands of an additional phase observed above 300 °C.

Phosphate modes

The infrared absorption peaks observed for the various phosphate vibrations are shown in Table 1. In this work we find the ν_1 modes of pseudomalachite at 996 and 978 cm^{-1}, the ν_2 modes at 448 and 416 cm^{-1}, and the ν_3 modes at 1095 and 1037 cm^{-1}. Bands observed for pseudomalachite at 612, 549, 525, and 478 cm^{-1} are attributed to the ν_4 vibrational modes. These values correspond well with the Raman spectra of these minerals (Frost et al. 2002). However, some disparity between these results and the published infrared absorption data is observed. For example, Farmer (1974) observed the ν_1 mode at 953 cm^{-1}. There is better agreement between the published infrared absorption data and the results reported here for the ν_2, ν_3, and ν_4 data. The observation of two sets of phosphate modes implies two different phosphate units in the molecular structure of pseudomalachite. Such a concept agrees well with the X-ray crystallographic data where two different phosphate units are observed in the unit cell.

For libethenite, two ν_1 absorption bands are observed at 955 and 917 cm^{-1}; the first value compares well with published result of 960 cm^{-1}. The Raman band is found at 975 cm^{-1}. The ν_3 band is found at 1031 cm^{-1}, a value that is less than the Raman

TABLE 2. Infrared emission spectral data of the hydroxyl-stretching region of pseudomalachite, libethenite, and cornetite

Precision of data	T(°C) +1 °C		100.0 +2 cm^{-1}	150.0 +2 cm^{-1}	200.0 +2 cm^{-1}	250.0 +2 cm^{-1}	300.0 +2 cm^{-1}	350.0 +2 cm^{-1}	400.0 +2 cm^{-1}	450.0 +2 cm^{-1}	500.0 +2 cm^{-1}
Pseudomalachite											
Band center/cm^{-1}		P_1	3021	2965	2959	2957	2958	3013	3045	3146	2999
Relative Intensity/%			19.6	12.7	12.1	10.5	9.6	9.9	9.6	16.9	39.3
Band center/cm^{-1}		P_2	3352	3259	3266	3277	3272	3299	3307	3366	3272
Relative Intensity/%			37.4	26.7	24.3	24.0	24.0	26.4	27.5	7.5	18.8
Band center/cm^{-1}		P_3	3382	3420	3387	3376	3370	3362	3356	3397	3412
Relative Intensity/%			12.6	37.6	25.4	22.5	20.7	15.1	12.5	50.5	28.3
Band center/cm^{-1}		P_4	3431	3441	3443	3440	3439	3435	3433	3430	3431
Relative Intensity/%			12.1	9.7	19.5	24.1	26.6	30.0	32.7	19.4	4.7
Band center/cm^{-1}		P_5	3440	3568	3545	3549	3554	3559	3564	3637	3595
Relative Intensity/%			18.4	13.4	18.7	19.0	19.2	18.6	17.7	5.6	8.9
Libethenite											
Band center/cm^{-1}		L_1	3230	3249	3243	3271	3271	3284	3277	3203	
Relative Intensity/%			6.2	7.8	6.5	7.2	7.1	8.0	8.5	5.6	
Band center/cm^{-1}		L_2	3411	3407	3397	3397	3394	3393	3390	3393	3366
Relative Intensity/%			19.9	19.8	19.3	18.5	19.3	19.2	21.7	30.8	28.9
Band center/cm^{-1}		L_3	3468	3466	3464	3462	3460	3458	3455	3454	3452
Relative Intensity/%			51.9	37.6	25.4	22.5	20.7	15.1	12.5	50.5	28.3
Band center/cm^{-1}		L_4	3540	3560	3549	3540	3537	3537	3539		
Relative Intensity/%			9.0	6.1	3.4	3.3	3.4	3.5	3.9		
Band center/cm^{-1}		L_5	3616		6.9	3613	3612	3612	3616		
Relative Intensity/%			13.0			6.1	5.9	6.0	0.6		
Band center/cm^{-1}		L_6		3624	3619	3625	3626	3626	3627		
Relative Intensity/%				6.3	2.6	1.4	1.3	1.2	1.0		
Band center/cm^{-1}		L_7		3689	3690	3687	3684	3681	3679	3634	3622
Relative Intensity/%					2.7	3.3	3.0	3.2	3.2	3.8	3.2
Cornetite											
Band center/cm^{-1}		C_1	2908	2494	2508	2494	2925	2590			
Relative Intensity/%			7.1	2.0	2.2	2.6	17.3	1.9			
Band center/cm^{-1}		C_2	3143	3039	3029	3041	3171	2864			
Relative Intensity/%			11.3	18.4	18.3	22.8	22.8	17.4			
Band center/cm^{-1}		C_3	3245	3283	3284	3290	3239	3142			
Relative Intensity/%			17.1	26.7	27.2	28.8	10.2	32.1			
Band center/cm^{-1}		C_4	3323	3331	3331	3331	3324	3241			
Relative Intensity/%			20.0	13.0	10.4	6.3	7.2	10.2			
Band center/cm^{-1}		C_5	3411	3411	3413	3415	3405	3323			
Relative Intensity/%			35.4	23.9	30.2	31.4	36.6	15.7			
Band center/cm^{-1}		C_6	3536	3495	3535	3556	3577	3414			
Relative Intensity/%			9.2	16.0	11.8	8.1	6.0	22.7			

result of 1050 cm^{-1}. Two ν_2 vibrations are observed at 448 and 420 cm^{-1}. The 448 cm^{-1} band corresponds well with the Raman results and with published data. Absorption bands at 648, 631, 610, and 548 cm^{-1} are attributed to the ν_4 modes with the degeneracy arising from loss of symmetry. Several bands were also observed in similar positions in the Raman spectra. For cornetite two IR absorption symmetric stretching modes were observed at 989 and 955 cm^{-1}. These values correspond well with the results of our Raman studies. The published value is at 960 cm^{-1}. The value for ν_3 seems to vary considerably depending on the technique used for measurement. Two bands were observed at 1093 and 1041 cm^{-1}, compared with the Raman result of 1054 cm^{-1}. Three absorption peaks were observed by Farmer (1974) at 1070, 1015, and 1000 cm^{-1}. Only a single absorption band for ν_2 of cornetite was observed at 452 cm^{-1}, compared with 462 cm^{-1} observed in the Raman spectrum and 464 cm^{-1} in the literature. Infrared absorption bands found at 618, 573, and 560 cm^{-1} are assigned to the ν_4 vibrational mode.

Infrared emission of the phosphate

The IES between 700 and 1800 cm^{-1} of the three basic copper phosphate minerals are shown in Figure 6. The infrared emission spectroscopy configuration only enables detection of bands above 650 cm^{-1}. In general, the results of the infrared emission spectra agree with the absorption data. The spectral definition, which is observed in the low wavenumber spectra taken over the 100 to 400 °C range, is lost above this temperature. In the 450 to 750 °C temperature range the spectra show no definition; however at higher temperatures increased definition is observed. The appearance of new bands at temperatures above 750 °C suggests that new phosphate phases are being generated.

Figure 7 displays the variation in peak intensity of the hydroxyl-bending bands as a function of temperature. The intensity of these bands parallels the loss of intensity of the hydroxyl-stretching bands and approaches zero by 450 °C. Other bands retain intensity up to quite high temperatures (Fig. 7).

For pseudomalachite three bands are observed at 885, 813, and 755 cm^{-1}, i.e., at energies associated with the OH-bending

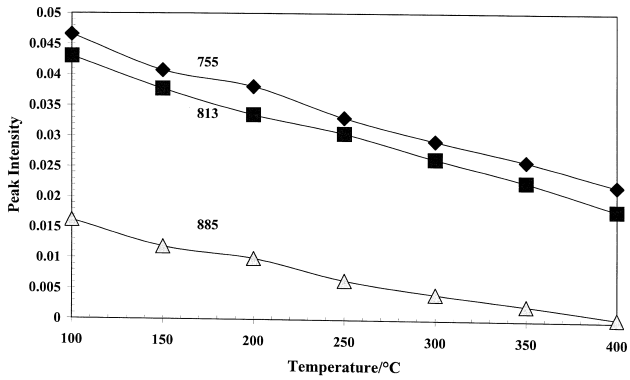

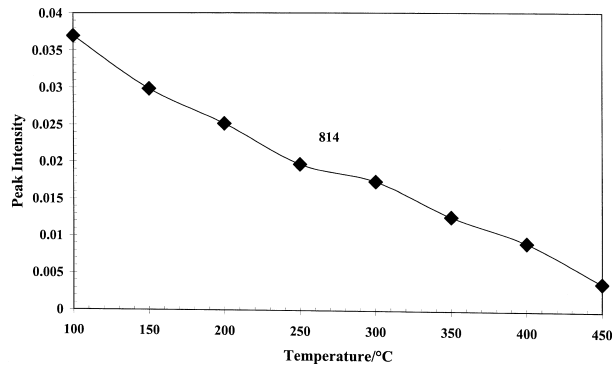

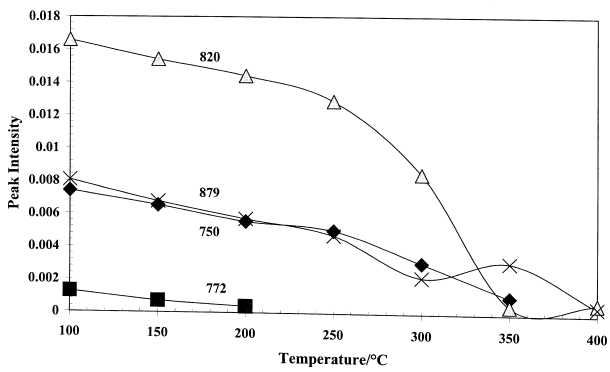

FIGURE 7. Intensity of the hydroxyl bending vibrations of (**a**) pseudomalachite, (**b**) libethenite, and (**c**) cornetite as a function of temperature.

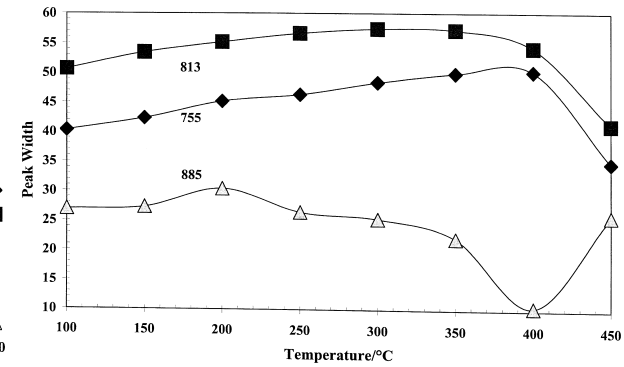

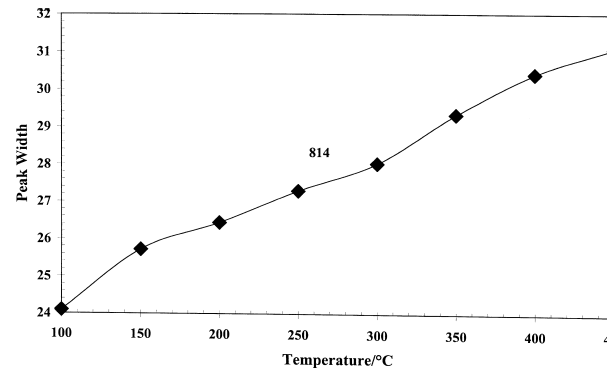

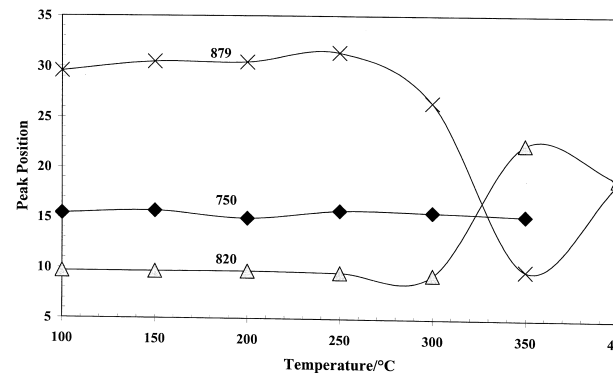

FIGURE 8. Peak width of the hydroxyl bending vibrations of (**a**) pseudomalachite, (**b**) libethenite, and (**c**) cornetite as a function of temperature.

vibrations based upon the position of these bands and a similar number of hydroxyl-stretching modes observed. These bands are assigned to the hydroxyl-bending vibrations.

For libethenite, the assignment is simpler. In parallel to the observation of one band of significant intensity in the hydroxyl-stretching region only one band is observed in the hydroxyl-bending region (at 814 cm^{-1}). The intensity of this band reaches zero by 450 °C. For cornetite four bands are observed in the 750 to 880 cm^{-1} region. The intensity of each of these bands approaches zero by 350 or 400 °C. These four modes correlate with the four hydroxyl-stretching modes supporting their assignment to the hydroxyl-bending vibrations. The variation in peak width shows the increase in bandwidth with increasing temperature (Fig. 8). When a basic copper phosphate phase undergoes a phase change such as dehydroxylation, discontinuities in peak width are observed. Such variation is illustrated over the 350 to 450 °C temperature range for both pseudomalachite and cornetite.

ACKNOWLEDGMENTS

The financial and infra-structure support of the Queensland University of Technology Centre for Instrumental and Developmental Chemistry is gratefully acknowledged. The Australian Research Council (ARC) is thanked for funding. P.A. Williams of the University of Western Sydney is thanked for much advice.

REFERENCES CITED

Anthony, J.W., Bideaux, B.R., Bladh, K.W., and Nichols, M.C. (2000) Handbook of Mineralogy Volume IV arsenates, phosphates and vanadates. Mineral Data Publishing, Tuscon, Arizona.

Braithwaite, R.S.W. and Ryback, G. (1994) Reichenbachite from Cornwall and Portugal. Mineralogical Magazine, 58, 449–51.

Farmer, V.C. (1974) Mineralogical Society Monograph 4: The Infrared Spectra of Minerals.

Frost, R.L. and Vassallo, A.M. (1996) The dehydroxylation of the kaolinite clay minerals using infrared emission spectroscopy. Clays and Clay Minerals, 44, 635–651.

——— (1997) Fourier-transform infrared emission spectroscopy of kaolinite dehydroxylation. Mikrochimica Acta, Supplement, 14, 789–791.

Frost, R.L., Collins, B.M., Finnie, K., and Vassallo, A.J. (1995) Infrared emission spectroscopy of clay minerals and their thermal transformations. Clays Controlling Environ., Procedings of the International Clay Conference, 219–24.

Frost, R.L., Kloprogge, J.T., Russell, S.C., and Szetu, J. (1999a) Dehydroxylation and the vibrational spectroscopy of aluminium (oxo)hydroxides using infrared emission spectroscopy. Part III: diaspore. Applied Spectroscopy, 53, 829–835.

——— (1999b) Dehydroxylation of aluminium (oxo)hydroxides using infrared emission spectroscopy. Part II: Boehmite. Applied Spectroscopy, 53, 572–582.

Frost, R. L., Williams, P. A., Martens, W. N., Kloprogge, J.T., and Leverett, P. (2002) Raman spectroscopy of the basic copper phosphate minerals cornetite, libethenite, pseudomalachite, reichenbachite and ludjibaite. Journal of Raman Spectroscopy, 33, 260–263.

Hyrsl, J. (1991) Three polymorphs of Cu5(PO4)2(OH)4 from Lubietova, Czechoslovakia. Neues Jahrbuch für Mineralogie, Monatshefte, 281–287.

Kloprogge, J.T. and Frost, R.L. (1999) Infrared emission spectroscopy of Al-pillared beidellite. Applied Clay Science, 15, 431–445.

——— (2000a) Infrared emission spectroscopy study of the dehydroxylation of 10 Å halloysite from a Neogene cryptokarst of southern Belgium. Geol. Belg., 2, 213–220.

——— (2000b) Study of the thermal behaviour of rectorite by in-situ infrared emission spectroscopy. Neues Jahrbuch für Mineralogie, Monatshefte, 145–157.

Lhoest, J.J. (1995) Famous mineral localities: the Kipushi Mine, Zaire. Mineralogical Record, 26, 163–92.

Moore, P.B. (1984) Phosphate Minerals. Springer-Verlag, Berlin.

Piret, P. and Deliens, M. (1988) Description of ludjibaite, a polymorph of pseudomalachite $Cu_5(PO_4)_2(OH)_4$. Bulletine de Mineralogie, 111, 167–171.

Sieber, N.H.W., Tillmanns, E. and Medenbach, O. (1987) Hentschelite, $CuFe_2(PO_4)_2(OH)_2$, a new member of the lazulite group, and reichenbachite, $Cu_5(PO_4)_2(OH)_4$, a polymorph of pseudomalachite, two new copper phosphate minerals from Reichenbach, Germany. American Mineralogist, 72, 404–408.

Williams, P.A. (1990) Oxide Zone Geochemistry. Ellis Horwood Ltd, Chichester, West Sussex, England.

MANUSCRIPT RECEIVED JANUARY 22, 2002
MANUSCRIPT ACCEPTED SEPTEMBER 24, 2002
MANUSCRIPT HANDLED BY JEFFREY E. POST